Solid-State ^{13}C NMR Reveals Annealing of Raft-Like Membranes Containing Cholesterol by the Intrinsically Disordered Protein α-Synuclein

Avigdor Leftin[1], Constantin Job[1], Klaus Beyer[1] and Michael F. Brown[1,2]

1 - Department of Chemistry and Biochemistry, *University of Arizona, Tucson, AZ 85721, USA*
2 - Department of Physics, *University of Arizona, Tucson, AZ 85721, USA*

Correspondence to Michael F. Brown: *mfbrown@u.arizona.edu*
http://dx.doi.org/10.1016/j.jmb.2013.04.002
Edited by A. G. Palmer III

Abstract

Misfolding and aggregation of the intrinsically disordered protein α-Synuclein (αS) in Lewy body plaques are characteristic markers of late-stage Parkinson's disease. It is well established that membrane binding is initiated at the N-terminus of the protein and affects biasing of conformational ensembles of αS. However, little is understood about the effect of αS on the membrane lipid bilayer. One hypothesis is that intrinsically disordered αS alters the structural properties of the membrane, thereby stabilizing the bilayer against fusion. Here, we used two-dimensional ^{13}C separated local-field NMR to study interaction of the wild-type α-Synuclein (wt-αS) or its N-terminal (1–25) amino acid sequence (N-αS) with a cholesterol-enriched ternary membrane system. This lipid bilayer mimics cellular raft-like domains in the brain that are proposed to be involved in neuronal membrane fusion. The two-dimensional dipolar-recoupling pulse sequence DROSS (dipolar recoupling on-axis with scaling and shape preservation) was implemented to measure isotropic ^{13}C chemical shifts and ^{13}C–^{1}H residual dipolar couplings under magic-angle spinning. Site-specific changes in NMR chemical shifts and segmental order parameters indicate that both wt-αS and N-αS bind to the membrane interface and change lipid packing within raft-like membranes. Mean-torque modeling of ^{13}C–^{1}H NMR order parameters shows that αS induces a remarkable thinning of the bilayer (≈6 Å), accompanied by an increase in phospholipid cross-sectional area (≈10 Å^2). This perturbation is characterized as membrane annealing and entails structural remodeling of the raft-like liquid-ordered phase. We propose this process is implicated in regulation of synaptic membrane fusion that may be altered by aggregation of αS in Parkinson's disease.
© 2013 Published by Elsevier Ltd.

Introduction

Parkinson's disease is a debilitating neurological disorder that increasingly afflicts the aging populations of industrialized countries.[1] The symptoms of the disease arise from neuronal cell death and are associated with a drastic impairment of the dopaminergic system.[2] A characteristic trait of Parkinson's disease is misfolding and aggregation of the protein α-Synuclein (αS). This intrinsically disordered protein undergoes a series of membrane-dependent conformational transitions[3] that may be implicated in neurodegeneration. Ultimately, αS aggregates into fibrillar plaques—known as Lewy bodies—that accumulate in dopaminergic neurons within the substantia nigra. Yet, the biological function of αS and its definitive connection to Parkinson's disease remain largely unknown.[4,5] One hypothesis for the function of αS is that it stabilizes synaptic membranes against fusion in the complex processes of neurotransmission that go awry during Parkinson's disease.[6,7] The current study aims to further investigate the structural correlates of this proposal, thus adding to our understanding of αS interactions with the raft-like neuronal membranes.

Chemical signaling in neurons is regulated by fusion of synaptic vesicles with the active zone of the nerve terminal plasma membrane.[8] The protein αS is known to exhibit specific interactions with the presynaptic membranes,[9–11] including small synaptic vesicles, and the presynaptic active zone. A hallmark feature of these membranes is compositional heterogeneity[12] involving both lipid species and phase behavior of the

Please cite this article as: Leftin, A. *et al.*, Solid-State ^{13}C NMR Reveals Annealing of Raft-Like Membranes Containing Cholesterol by the Intrinsically Disordered Protein α-Synuclein, *J. Mol. Biol.* (2013), http://dx.doi.org/10.1016/j.jmb.2013.04.002

UNCORRECTED PROOF

ARTICLE IN PRESS

Q2

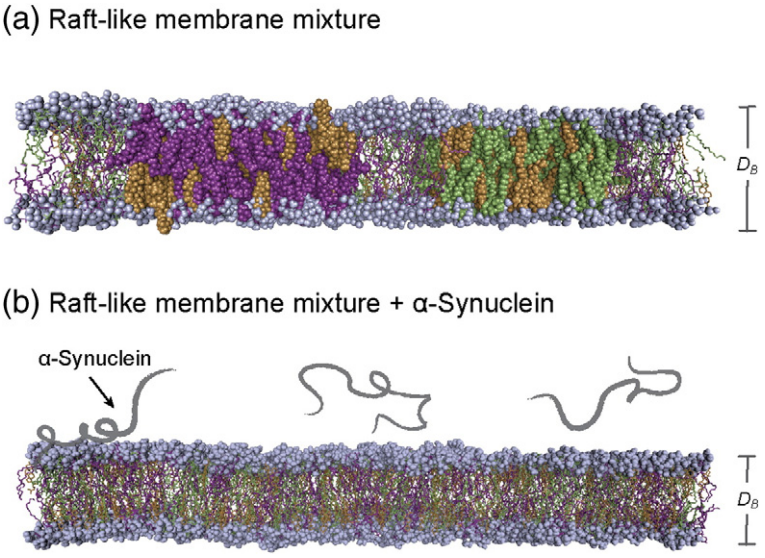

Fig. 1. Membrane model shows biophysical mechanism for how αS interacts with synaptic vesicle lipids. αS is a presynaptic neuronal protein found in Lewy bodies that occur in Parkinson's disease. The proposed annealing of raft-like membrane defects by αS is depicted. (a) Raft-based membranes constitute a heterogeneous system that is non-ideally mixed on the nanometer scale. Clusters of POPC lipids (purple) or EYSM lipids (green) with cholesterol (Chol; brown) coexist with mixed POPC/EYSM/Chol regions, giving rise to local membrane defects. (b) Natively unfolded αS binds to raft-like defects due to sphingomyelin and cholesterol. Annealing by αS involves transient association with interfacial sites, which perturbs stabilizing lipid packing interactions. Changes in the hydrophobic membrane environment entail remodeling of the liquid-ordered (l_o) phase of POPC and EYSM with cholesterol, yielding a liquid-disordered (l_d) phase with a smaller bilayer thickness (D_B).

bilayers. In particular, a key feature promoting the interaction of αS with membranes is the presence of detergent-insoluble microdomains (rafts)—coexistence regions of liquid-disordered (l_d) and liquid-ordered (l_o) lipid phases—that are favored by the presence of cholesterol, sphingomyelin, and unsaturated lipids.[13–15] Binding of αS to raft-like membranes and curved single-phase bilayers is initiated by association of the N-terminal consensus sequence (N-αS) with the membrane interface, leading to a coil–helix conformational transition of the protein.[16] Association of αS to such membranes yields an inhibition of vesicle fusion that involves a general restructuring of the lipid membrane by modulating membrane curvature,[17] so as to remove lateral phase defects in compositionally or topologically heterogeneous systems.[7,16,18–20] These observations underlie our hypothesis that αS fulfills a regulatory function in synaptic neurotransmission by structurally remodeling neuronal raft-like membranes (Fig. 1).

In this article, we focus on the interaction of wild-type α-Synuclein (wt-αS) and N-αS with a canonical raft-like mixture comprising 1-palmitoyl-2-oleoyl-*sn*-glycero-3-phosphocholine (POPC), egg yolk sphingomyelin (EYSM), and cholesterol (Chol) using solid-state NMR spectroscopy.[21] We characterize the membrane lipid behavior upon association of αS by two-dimensional (2D) separated local-field (SLF) NMR under magic-angle spinning (MAS). The SLF experiment DROSS (dipolar recoupling on-axis with scaling and shape preservation)[22] permits site-specific and simultaneous measurements of ^{13}C isotropic chemical shifts and ^{13}C–^{1}H residual dipolar couplings (RDCs) of the headgroup, backbone, and acyl chains of the membrane phospholipids.[21,23–28] An important aspect is that isotopic enrichment is not required, thus providing a distinct advantage over complementary solid-state ^{2}H NMR experiments.[29,30] Using our approach, the isotropic ^{13}C chemical shifts and RDCs monitor association of both truncated N-αS and wt-αS with the lipid membrane interface. We show that this experiment reveals large structural changes in the hydrocarbon region of the membrane. The ^{13}C–^{1}H RDCs are evaluated in terms of ^{13}C–^{1}H segmental order parameters (S_{CH}) using a simple mean-torque model for bilayer structural properties.[31] Both the full-length protein and the N-terminal αS peptide elicit disorder in the phospholipid hydrocarbon chains, resulting in thinning of the raft-like lipid membranes. Binding of αS acts oppositely to cholesterol because it anneals the ordered raft-like membranes. In the context of Parkinson's disease, raft-like membrane lipids may play an important role in regulatory neurotransmitter release. The remodeling or annealing of the raft-like phase observed by solid-state ^{13}C NMR addresses a molecular mechanism suggested by previous research, whereby αS stabilizes membranes against fusion. A corollary is that misfolding and aggregation of αS into toxic oligomers may lead to defective membrane remodeling and therefore misregulation of membrane fusion giving rise to symptoms of Parkinson's disease.

Results

2D SLF ^{13}C NMR experiments probe membrane lipids at natural isotopic abundance

The 2D ^{13}C–^{1}H correlation experiment DROSS targets membrane components exclusively at ^{13}C

UNCORRECTED PROOF

Please cite this article as: Leftin, A. *et al.*, Solid-State ^{13}C NMR Reveals Annealing of Raft-Like Membranes Containing Cholesterol by the Intrinsically Disordered Protein α-Synuclein, *J. Mol. Biol.* (2013), http://dx.doi.org/10.1016/j.jmb.2013.04.002

ARTICLE IN PRESS

Q2

natural isotopic abundance. MAS allows one to investigate site-specific features and phase characteristics of complex biomembrane systems, without the need of isotopic labeling as required in ^{2}H NMR spectroscopy.[32–39] Thus far, the DROSS experiment has been implemented for the benchmark saturated glycerophospholipid DMPC,[22] for mixtures of the symmetric monounsaturated glycerophospholipid DOPC with cholesterol,[25] and for polyunsaturated lipid species.[39] To further test the performance of DROSS on the asymmetric glycerophospholipid POPC and the sphingolipid EYSM, we recorded 2D spectra and extracted the ^{13}C NMR isotropic chemical shifts and ^{13}C–^{1}H RDC lineshapes for these components in raft-like membrane lipid mixtures. Figure 2a shows the structures and carbon assignments for the POPC and EYSM phospholipids. The respective single-component data sets obtained at 48 °C are shown in Fig. 2b and c where both phospholipids are in the l_d phase. This temperature is ≈10 °C above the solid-ordered (s_o) to l_d phase transition temperature T_M of EYSM bilayers. The DROSS experiment is restricted to experiments conducted above the T_M of lipid membranes due to the inefficiency of the INEPT magnetization transfer in s_o systems. The chemical shift spectra report on the nonpolar bilayer interior (0–45 ppm), the polar aqueous interfacial region (50–80 ppm), and sites of unsaturation of the acyl chain (115–135 ppm). The large chemical shift dispersion allows unique assignments to be made for the entire phospholipid molecules, which is not the case in ^{2}H NMR spectroscopy. Large differences in breadth of the RDC lineshapes for each of the isotropic chemical shift positions are observed for both POPC and EYSM phospholipids. Note that the RDCs of EYSM are larger than those of POPC, as a consequence of greater acyl chain ordering and the

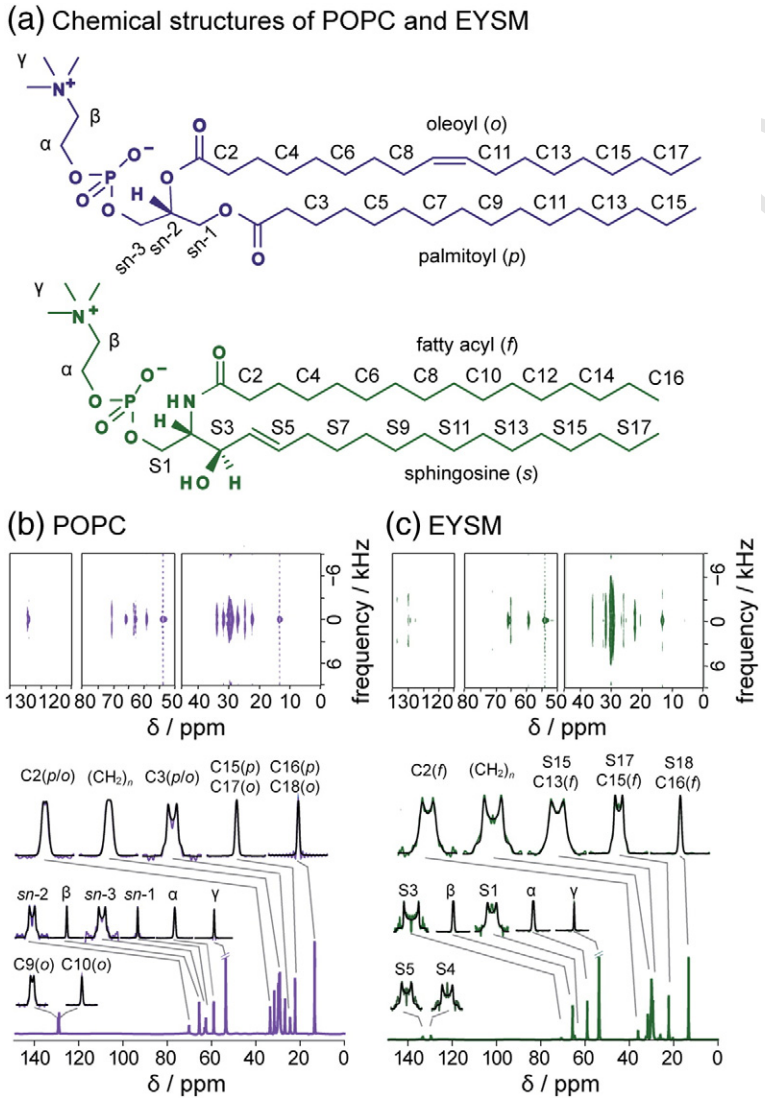

Fig. 2. SLF ^{13}C NMR investigates raft-forming EYSM and POPC phospholipids at natural isotopic abundance. (a) Chemical structures of the glycerophospholipid POPC having palmitoyl (*p*) and oleoyl (*o*) chains, and sphingolipid EYSM with fatty acyl (*f*) and sphingosine (*s*) chains. 2D dipolar-recoupled NMR spectra obtained under MAS at 48 °C are shown for (b) POPC and (c) EYSM bilayers. Spectral planes are assigned to unsaturated (115–135 ppm), headgroup plus backbone (50–80 ppm), and acyl chain (0–40 ppm) resonances. Both phospholipids are in the liquid-disordered (l_d) phase. Site-specific differences of ^{13}C isotropic chemical shifts and ^{13}C–^{1}H RDCs indicate the applicability of using the DROSS pulse sequence to follow these spectral features in complex raft-like ternary membranes at natural ^{13}C isotopic abundance.

Please cite this article as: Leftin, A. *et al.*, Solid-State ^{13}C NMR Reveals Annealing of Raft-Like Membranes Containing Cholesterol by the Intrinsically Disordered Protein α-Synuclein, *J. Mol. Biol.* (2013), http://dx.doi.org/10.1016/j.jmb.2013.04.002

ARTICLE IN PRESS

Q2

higher order–disorder transition temperature T_M (POPC, −2 °C; EYSM, 38 °C). Interactions responsible for the difference in the chain melting transition temperatures are attributed to van der Waals contacts and hydrogen bonding, in accord with ^{2}H NMR experiments.[30,40–42]

Raft-like phase coexistence in ternary lipid membranes is evident from solid-state ^{13}C NMR spectroscopy

An equimolar mixture of the phospholipids POPC and EYSM with cholesterol is useful as a paradigm for raft-forming membranes. This ternary membrane exhibits biphasic, fluid–fluid (liquid-ordered, l_o; liquid-disordered, l_d) phase coexistence over broad temperature and compositional ranges, according to fluorescence spectroscopy and small-angle X-ray scattering.[43–46] In addition, solid-state ^{2}H NMR has resolved the spectral signatures of cholesterol-enriched POPC and EYSM in distinct microenvironments.[30,42]

We performed the DROSS experiment to further characterize the behavior of the raft-like membrane lipids in aqueous dispersions prior to investigating the αS-ternary interaction system. Figure 3a shows the 2D SLF spectrum obtained at 48 °C for the raft-like mixture. The ^{13}C–^{1}H RDC lineshape projections and isotropic ^{13}C NMR chemical shifts from the 2D SLF experiment are shown in Fig. 3b. In the ^{13}C solid-state NMR experiments, the chemical shift interval between 29 and 32 ppm is associated with the $(CH_2)_n$ acyl chain segments. The broad spectral region in this instance reports on the heterogeneous raft-like microenvironments of the ternary lipid mixture. These domains are attributed to locally enriched pools of POPC or EYSM with cholesterol.[14,43,47–49] To substantiate the compositional heterogeneity of this system, next we obtained reference ^{13}C NMR chemical shift spectra for binary POPC/Chol, EYSM/Chol, and POPC/EYSM membranes corresponding to the microdomain environments. These binary mixtures provide a basis for interpreting the chemical shifts and for assessing the mixing behavior of the lipids in the ternary system.[40,41,50–55]

In order to demonstrate the sensitivity of the ^{13}C NMR experiment to compositional phase behavior,

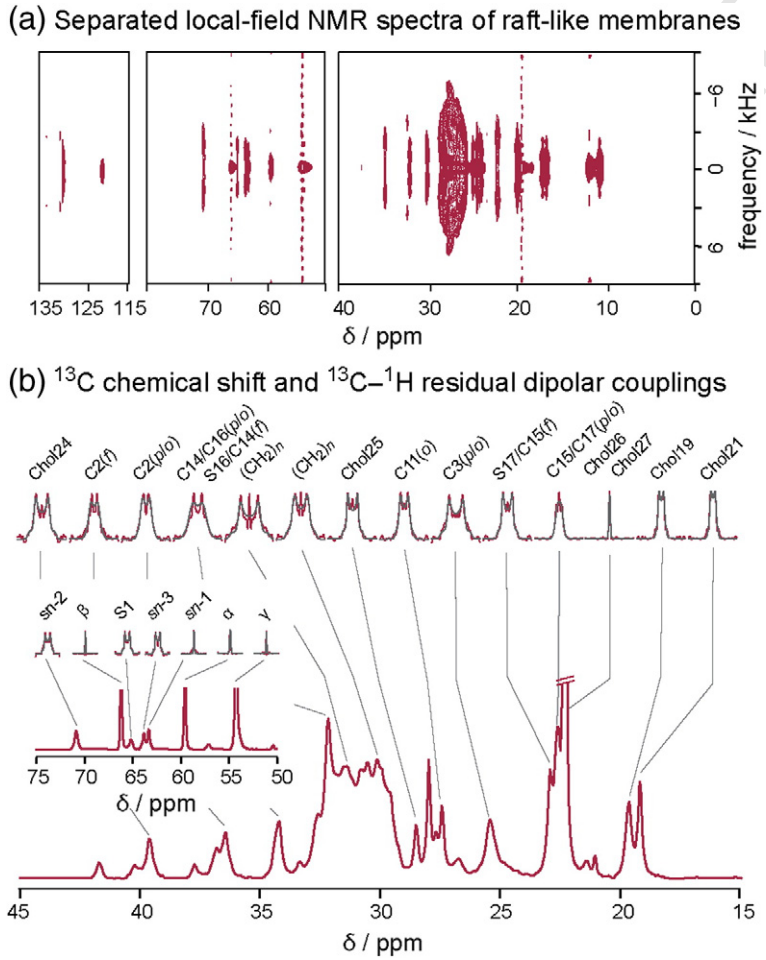

Fig. 3. Dipolar-recoupled ^{13}C NMR spectra of POPC/EYSM/Chol raft-like membranes. (a) Site-resolved 2D DROSS NMR spectra are shown for raft-like POPC/EYSM/Chol (1:1:1) lipid membranes at 48 °C. Spectral planes include unsaturated (115–135 ppm), headgroup plus backbone (50–80 ppm), and acyl chain (0–40 ppm) resonances of the phospholipids and cholesterol. (b) Experimental ^{13}C–^{1}H residual magnetic dipolar lineshapes and theoretical fits are shown together with ^{13}C NMR chemical shift projections for raft-like membranes and resonance assignments (cf. Fig. 2a).

Please cite this article as: Leftin, A. *et al.*, Solid-State ^{13}C NMR Reveals Annealing of Raft-Like Membranes Containing Cholesterol by the Intrinsically Disordered Protein α-Synuclein, *J. Mol. Biol.* (2013), http://dx.doi.org/10.1016/j.jmb.2013.04.002

ARTICLE IN PRESS

we show in Fig. 4 the ^{13}C chemical shift spectra in the range 15–45 ppm for these systems, corresponding to the central bilayer region. Additional spectral details for the mixed lipid systems are found in Figs. S1–S3 of Supplementary Data, and tabulations are given in Tables S1–S8. The binary EYSM/POPC system exhibits a spectrum resembling the superposition of single-component spectra, consistent with the presence of demixed sphingolipid and glycerolipid components.[43] The binary POPC/Chol and EYSM/Chol spectra exhibit distinct polymethylene regions that arise from heterogeneous phospholipid–phospholipid and phospholipid–cholesterol interactions within the l_o sphingolipid and glycerolipid pools. Linear combination of the binary spectra reproduces the salient features of the ternary spectrum recorded at 48 °C. Here, the POPC and EYSM polymethylene chemical shift regions yield significant contributions to the ternary membrane spectrum. This observation suggests that spectral overlap of the $(CH_2)_n$ region is due to chemical shift nonequivalence arising from heterogeneous phospholipid–phospholipid and phospholipid–cholesterol microenvironments of the POPC and EYSM lipid systems.

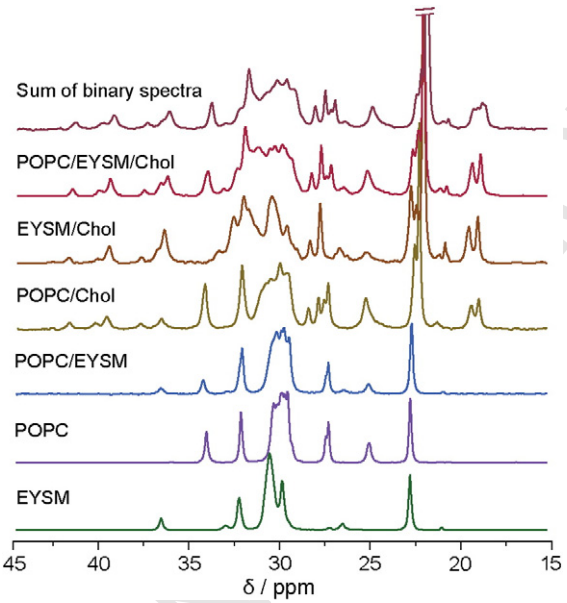

Fig. 4. Isotropic ^{13}C NMR chemical shift spectra demonstrate heterogeneity of raft-like membranes. ^{13}C INEPT-MAS NMR spectra are for single-component POPC and EYSM, as well as mixtures of EYSM/Chol (1:1), POPC/Chol (1:1), EYSM/POPC (1:1), and ternary POPC/EYSM/Chol (1:1:1) mixtures obtained at 48 °C. Note that the sum of binary spectra (1:1:1 linear combination) reproduces the raft-like POPC/EYSM/Chol (1:1:1) ternary spectrum. The spectral agreement supports the presence of cholesterol-enriched POPC and EYSM domains in the compositionally heterogeneous bilayer.

Natural abundance ^{13}C chemical shifts indicate selective interactions of αS with raft-like lipid membranes

It has been reported that αS interacts preferentially at biomembrane interfaces,[56–58] leading to structuring of the protein due to a coil–helix transition. Isotropic ^{13}C chemical shifts recorded in the 2D DROSS correlation spectra at 48 °C presented in Fig. 5a show that monomeric αS causes a significant spectral change, both within the membrane and at the membrane interface of the ternary POPC/EYSM/Chol (1:1:1) system. Notably, our experiment does not resolve ^{13}C chemical shifts for natural abundance sites of N-αS and wt-αS in the protein/lipid ratio used (1:250). Further, the INEPT polarization transfer of the DROSS pulse sequence was found to be ineffective for the majority of cholesterol sites, precluding meaningful analysis of these resonances. Therefore, we focus solely on POPC and EYSM in this system. Striking differences between the 29–32 ppm $(CH_2)_n$ region in the raft-like mixture alone (Fig. 3b) and in the presence of wt-αS (Fig. 5b) are observed. In this range, the chemical shift overlap is greatly reduced, giving a spectrum that resembles that recorded for the lipids in binary membranes (Fig. 4). These chemical shift changes are nearly identical for both the wt-αS and N-αS species (see Figs. S3 and S4 of Supplementary Data). Site-specific evidence for interfacial association is provided by a unique change at the α position of the choline headgroup, common to both POPC and EYSM phospholipids, in the presence of the wt-αS (Fig. 5b). We observe two peaks at 59.8 and 59.5 ppm, suggesting two magnetically or chemically distinct populations. The resonances may be tentatively assigned to αS-bound and unbound fractions of the lipid pool. An estimate of the lifetimes for these two states is obtained from $1/\Delta\delta = 26$ ms, where $\Delta\delta$ is the difference in chemical shift of the two resonance lines. The choline α carbon position is proximal to the phosphate group and is the site of phospholipase D conversion of glycerophospholipids to phosphatidic acid and choline. Such a site-specific marker of the interaction of wt-αS with the membrane may be a corollary of the phospholipase D inhibition by αS shown previously in biochemical studies.[59] However, this α-splitting does not occur with the N-αS peptide, suggesting that interactions between the protein and peptide with the membrane interface are not equivalent, which can be ascribed to the reduced binding partition coefficient of the small peptide compared to the full-length protein.[16] Differences in the degree and lifetime of this specific interfacial association can arise from contributions of the unstructured C-terminus, additional lysine-enriched repeats of the wild-type protein, and the hydrophobic sequence domain referred to as non-amyloid beta component (residues 61–95). The

UNCORRECTED PROOF

Please cite this article as: Leftin, A. *et al.*, Solid-State ^{13}C NMR Reveals Annealing of Raft-Like Membranes Containing Cholesterol by the Intrinsically Disordered Protein α-Synuclein, *J. Mol. Biol.* (2013), http://dx.doi.org/10.1016/j.jmb.2013.04.002

ARTICLE IN PRESS

Q2

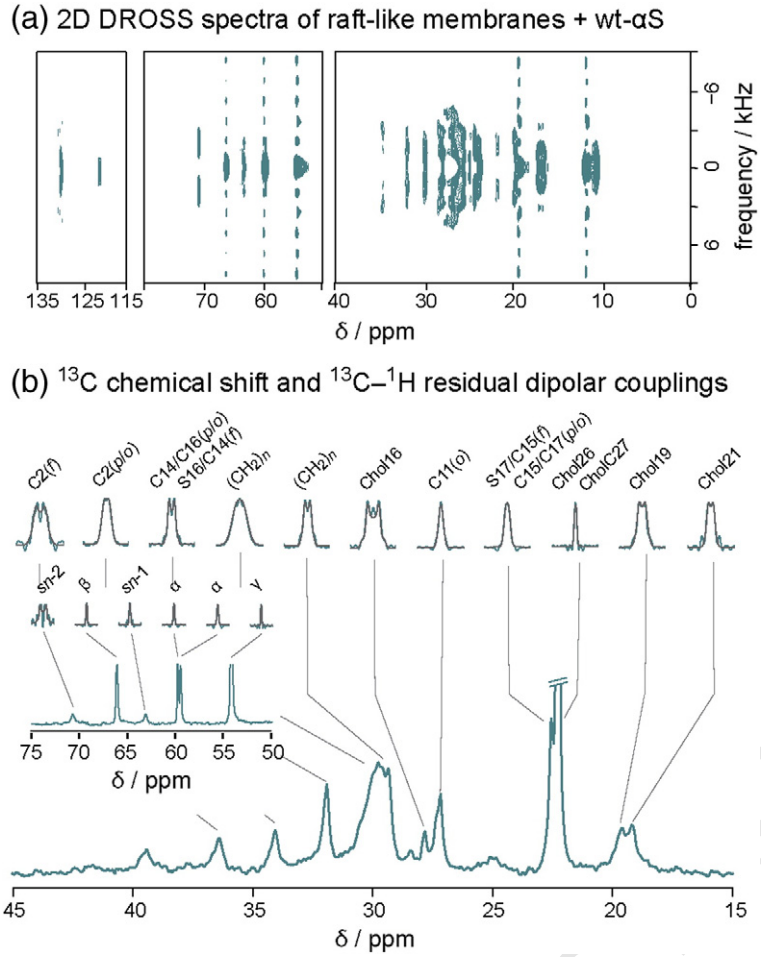

Fig. 5. SLF NMR reveals αS interactions with raft-like lipid membranes. (a) 2D ^{13}C chemical shift dipolar coupling correlation spectra for raft-like POPC/EYSM/Chol (1:1:1) membrane lipids containing wt-αS (protein/lipid molar ratio 1:250) at 48 °C. Spectral planes correspond to unsaturated sites (115–135 ppm), headgroup plus backbone (50–80 ppm), and saturated carbon segments of phospholipids and cholesterol (0–40 ppm), and exhibit pronounced differences compared to raft-like spectra in Fig. 3. (b) Isotropic ^{13}C chemical shifts (below) and ^{13}C–^{1}H dipolar lineshapes (above) extracted from 2D planes. Resonance assignments correspond to Fig. 2a.

latter has a critical role for nucleation of the aggregation process,[60] which has been shown in solid-state MAS NMR measurements to involve binding to lipid membranes.[61]

RDCs and order parameters from solid-state ^{13}C–^{1}H NMR spectroscopy reveal membrane perturbation by αS

From the 2D DROSS spectra, we extracted slices corresponding to RDC lineshapes of the chemically shifted resonance positions. The experimental and fitted RDC spectra in Fig. 6a and b are shown for selected headgroup and acyl chain positions, respectively. Note that the narrow RDC lineshapes of the phosphocholine headgroup *increase* in breadth in the presence of αS, while the acyl chain RDCs *decrease*. The interfacial RDC lineshapes are well above the isotropic limit, and increases of the RDCs indicate that the angular averaging of these segmental positions is reduced, or that the average conformation is changed through interfacial association. Another indication of this interaction is the baseline oscillations of the headgroup RDC lineshapes (Fig. 6a). Periodic artifacts arise from truncation of the free induction decay prior to Fourier transformation when long spin–spin relaxation times of the segments are present. The long relaxation times reflect greater isotropic motion of the headgroup sites. Upon interaction with αS, the truncation oscillations are diminished in frequency, suggesting an increased local-field magnetic dipolar contribution to the transverse nuclear spin relaxation from peptide and protein binding. The residual magnetic dipolar couplings of the raft-like membrane acyl chains without αS are characteristic of liquid-ordered, cholesterol-rich membrane phases, as seen in corresponding solid-state ^{2}H NMR studies that afford higher resolution of individual segments within the chain region.[30] In contrast to the increase of headgroup RDCs, for these chain positions, the presence of both the wt-αS protein and N-αS peptide leads to a reduction of the breadth of the RDC linewidth, suggesting that disordering of the chains occurs. This hitherto unobserved change accompanying the binding of αS is addressed in detail below.

To further characterize the structural perturbation at all resolved phospholipid positions and evaluate the local changes at the nonpolar hydrocarbon, backbone, and headgroup regions caused by αS, we

UNCORRECTED PROOF

Please cite this article as: Leftin, A. *et al.*, Solid-State ^{13}C NMR Reveals Annealing of Raft-Like Membranes Containing Cholesterol by the Intrinsically Disordered Protein α-Synuclein, *J. Mol. Biol.* (2013), http://dx.doi.org/10.1016/j.jmb.2013.04.002

ARTICLE IN PRESS

Q2

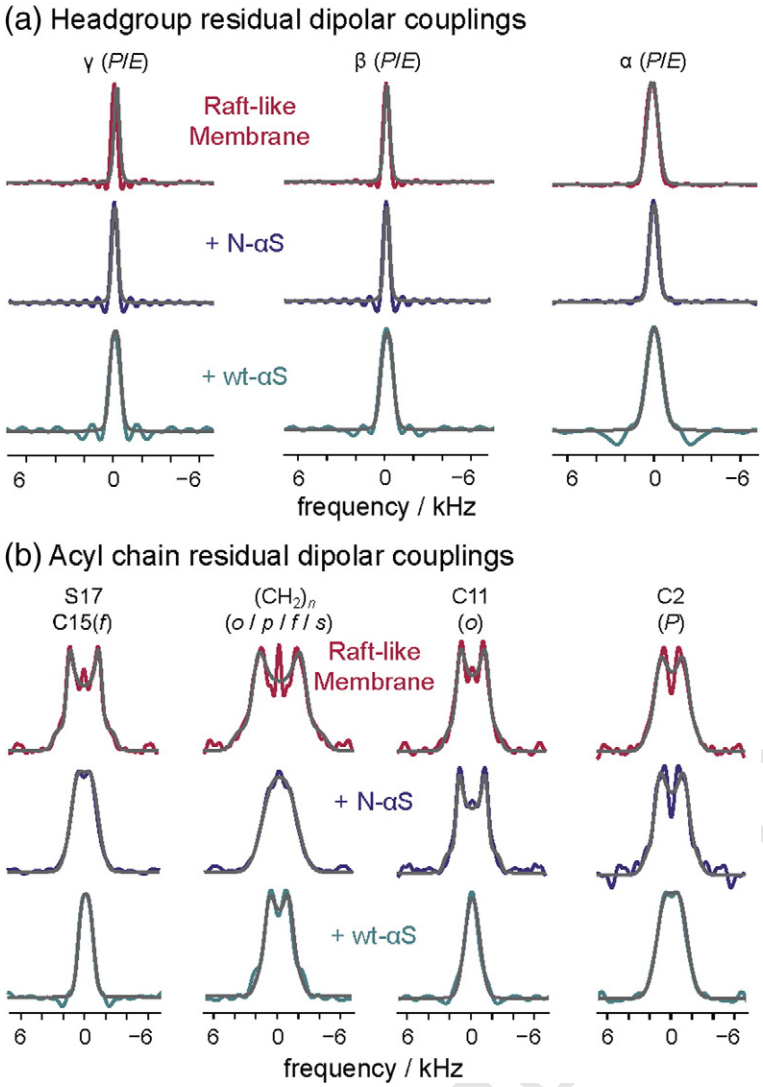

Fig. 6. Experimental $^{13}C–^{1}H$ residual dipolar couplings indicate wt-αS and N-αS interactions with raft-like membrane phospholipids. (a) Experimental $^{13}C–^{1}H$ DROSS dipolar lineshapes and theoretical fits for phosphocholine α, β, and γ headgroup positions of POPC (*P*) and EYSM (*E*) at 48 °C in the presence of wt-αS and N-αS (protein/lipid molar ratio 1:250). The increase in RDCs for headgroup positions is due to αS interaction. (b) RDCs of palmitoyl (*p*), oleoyl (*o*), fatty acyl (*f*), and sphingosine (*s*) chains of POPC and EYSM in raft-like membranes in the presence of wt-αS and N-αS at 48 °C. Note that for the acyl chains, there is a decrease in RDCs due to membrane interaction with αS.

summarize in Fig. 7 the RDCs as order parameter profiles of $|S_{CH}|$ *versus* carbon position. These profiles allow for site-specific evaluation of peptide and protein-induced changes to phospholipids that may be probed in both the SLF and ^{2}H NMR experiments.[28,62–64] In general, cholesterol order parameters of ring carbons are also expected to change as a function of membrane environment, though in the DROSS experiment, we could not accurately measure these values due to inefficiency of the INEPT polarization transfer at rigid cholesterol sites. Focusing on the phospholipids, the absolute ^{13}C NMR order parameter profiles of EYSM and POPC show that in the presence of αS, the interfacial S_{CH} values *increase* while the acyl chain S_{CH} values *decrease*. The observation of these changes substantiates that αS interacts with the biomembrane interface and leads to disordering of the hydrocarbon chains, oppositely to the effect of cholesterol in the raft-like system (see below).

To interpret the changes in $|S_{CH}|$ for the raft-like membranes, we obtained the absolute order parameter profiles for single-component and binary phospholipid/phospholipid and phospholipid/Chol membranes. The large differences of the POPC and EYSM single-component order parameters are due to the phase behavior and chemical properties of the lipids (see Supplementary Data). Mixing of POPC and EYSM causes an increase in the values of $|S_{CH}|$ for POPC and a decrease for EYSM. In the single-component and binary POPC/EYSM dispersions, the S_{CH} values indicate that the membrane lipids are in the l_d phase. For binary POPC/Chol and EYSM/Chol membranes, cholesterol acts to condense the lipids, yielding similar large order parameters for both POPC and EYSM in l_o phases (Fig. 7). The absolute order parameters for membrane lipids in the raft-like ternary system are similarly large, indicating cholesterol-enriched l_o lipid pools. Compared with these lipid membrane order parameter

Please cite this article as: Leftin, A. *et al.*, Solid-State ^{13}C NMR Reveals Annealing of Raft-Like Membranes Containing Cholesterol by the Intrinsically Disordered Protein α-Synuclein, *J. Mol. Biol.* (2013), http://dx.doi.org/10.1016/j.jmb.2013.04.002

ARTICLE IN PRESS

Q2

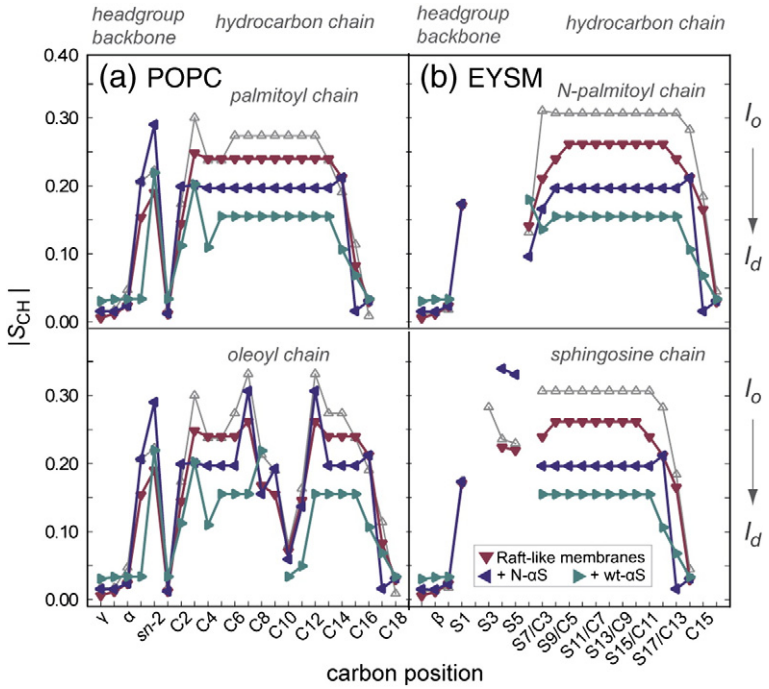

Fig. 7. Segmental order profiles characterize annealing of raft-like phospholipid ternary mixture by αS. Order parameters $|S_{CH}|$ (absolute magnitude) are plotted against carbon position for (a) POPC and (b) EYSM in (▾) ternary POPC/EYSM/Chol (1:1:1), (◂) POPC/EYSM/Chol (1:1:1) + N-αS, and (▸) POPC/EYSM/Chol + wt-αS membrane mixtures at 48 °C (protein/lipid molar ratio 1:250). Interfacial αS association with lipid sites produces large-scale structural changes throughout the hydrophobic acyl chain region. Order parameters are compared to liquid-ordered (△) phospholipid/Chol (1:1) mixtures. The results support αS-induced changes from liquid-ordered to liquid-disordered states.

profiles, the phospholipid chains in raft-like mixtures containing wt-αS and N-αS exhibit order parameters trending towards lower $|S_{CH}|$ values characteristic of the l_d phase. As noted above, this decrease is opposite to the increase of phospholipid order parameters caused by cholesterol. A possible cause of the change in order parameters is a disordering of the raft-like l_o membrane hydrocarbon environment, leading to an l_d-like phase, which is also supported by the change in appearance of the chemical shift spectrum of the ternary lipid system in the presence of αS or N-αS. Thus, we propose that αS antagonizes the condensing and ordering effect that cholesterol has on phospholipids through a disordering mechanism presented in the Discussion.

The change of interfacial order parameters lends further insight into the disordering function of the protein. For the phosphocholine headgroup α, β, γ segments, the order parameters increase in the presence of wt-αS and N-αS, indicating that both the N-terminal peptide and full-length protein interact with the membrane interface.[16,58,65,66] Moreover, the order parameters for the glycerol *sn*-1, *sn*-2, and *sn*-3 positions (Fig. 7a), as well as the resolved sphingosine S4 and S5 segments (Fig. 7b), increase in the presence of both N-αS and wt-αS. As an estimate of the depth of αS penetration into the membrane, the headgroup thicknesses for glycerolipids and sphingolipids are 9 Å and 7 Å, respectively. These thicknesses can be approximately separated into phosphocholine (≈3–4 Å) and backbone (≈7–9 Å) depths. In the case of wt-αS, the change of order parameter is greatest at the zwitterionic phosphocholine headgroup, suggesting that the protein is approximately localized to the upper <3–4 Å region of the bilayer. For N-αS, order parameters of the glycerol backbone and the segmental sites proximal to interfacial hydrogen bonding sites of EYSM are affected more than the headgroup, indicating further penetration to <7–9 Å into the bilayer interface. Such changes at the l_o membrane interface may involve disruptions of hydrogen bonding for EYSM and close packing of lipids for both POPC and EYSM. These interactions contribute to the raft-like heterogeneity of the ternary membrane,[47–49] and their disruption can facilitate alteration of van der Waals hydrophobic contacts in the bilayer core leading to l_d states.

The intrinsically disordered protein αS remodels raft-like membranes containing cholesterol

Local molecular perturbations as discussed above can also give rise to larger-scale changes in membrane structure. These changes may be characterized according to two structural quantities derived from the segmental S_{CH} order parameters obtained at uniquely resolved chemical shift sites of the phospholipid hydrocarbon chains using the mean-torque model.[31] The first quantity is the average cross-sectional area $\langle A_C \rangle$ and the second is the volumetric hydrocarbon thickness per phospholipid chain D_C. For a given phospholipid type, the value of $2D_C$ gives the overall thickness of the membrane bilayer D_B, neglecting headgroup contributions D_H for the monolayer leaflets. In addition, the total interfacial cross-sectional area per phospholipid may be estimated as $2\langle A_C \rangle = \langle A \rangle$, since order

UNCORRECTED PROOF

Please cite this article as: Leftin, A. *et al.*, Solid-State ^{13}C NMR Reveals Annealing of Raft-Like Membranes Containing Cholesterol by the Intrinsically Disordered Protein α-Synuclein, *J. Mol. Biol.* (2013), http://dx.doi.org/10.1016/j.jmb.2013.04.002

ARTICLE IN PRESS

parameters of both chains at the membrane interface are treated equivalently in the NMR data reduction. Any perturbation affecting hydrogen bonding, electrostatics, or van der Waals interactions of the membrane lipids yields a change in S_{CH} and will alter the structural quantities accordingly. The $\langle A_C \rangle$ and D_C values are presented in Fig. 8a and b, respectively, for the αS-containing raft-like mixtures, as well as the ternary raft-like mixture at 48 °C (see Table S13). The $\langle A_C \rangle$ and D_C results for binary l_o and l_d phases at 48 °C are also shown to assist in understanding the structural perturbation of the raft-like membrane caused by αS interaction.

By applying the mean-torque model,[31] the cross-sectional areas determined for each phospholipid in the raft-like membrane mixture are found to be $\langle A \rangle$ = 57.6 Å^2 for POPC and $\langle A \rangle$ = 56.4 Å^2 for EYSM. The slightly smaller cross-sectional area for EYSM reflects larger contributions to inter-lipid packing due to hydrogen bonding and favorable hydrophobic matching between saturated chains. These cross-sectional areas per phospholipid compare closely with ^{2}H NMR values determined for perdeuterated *sn*-1 palmitoyl chains[30] and also monolayer measurements obtained at 30 mN/m surface tension for the same raft components.[67,68] For POPC in the raft-like system, D_C values of 15.6 Å and 17.1 Å are found for the palmitoyl (16:0) and oleoyl (18:1, *cis*-Δ^9) chains, respectively, at 48 °C (Fig. 8b). The fatty acyl chain of EYSM (*N*-palmitoyl, 16:0, predominant species ≈ 86%[69]) in the ternary membrane has a D_C value of 15.9 Å. We calculated D_C for the sphingosine chain assuming an effective 16:1, *trans*-Δ^2 chain giving D_C = 15.4 Å at 48 °C in the ternary mixture. By considering symmetric bilayer leaflets, and including estimates of headgroup and backbone dimensions D_H, the mixed membrane system has nonequivalent bilayer thickness contributions of $D_B \approx 52.2$ Å for POPC and for $D_B \approx 45.8$ Å for EYSM. This reflects the larger glycerol backbone thickness compared with the sphingosine backbone, as well as the longer 18:1, *cis*-Δ^9 hydrocarbon chain length of the oleoyl chain compared with the 16:1, *trans*-Δ^2 sphingosine chain of EYSM. These bilayer thicknesses and cross-sectional areas point to an equilibrium distribution of cholesterol-enriched, condensed complexes of lipids[70] in liquid-ordered phases, similar to the binary phospholipid/cholesterol systems presented in Fig. 8, which possess different phospholipid hydrophobic thicknesses.

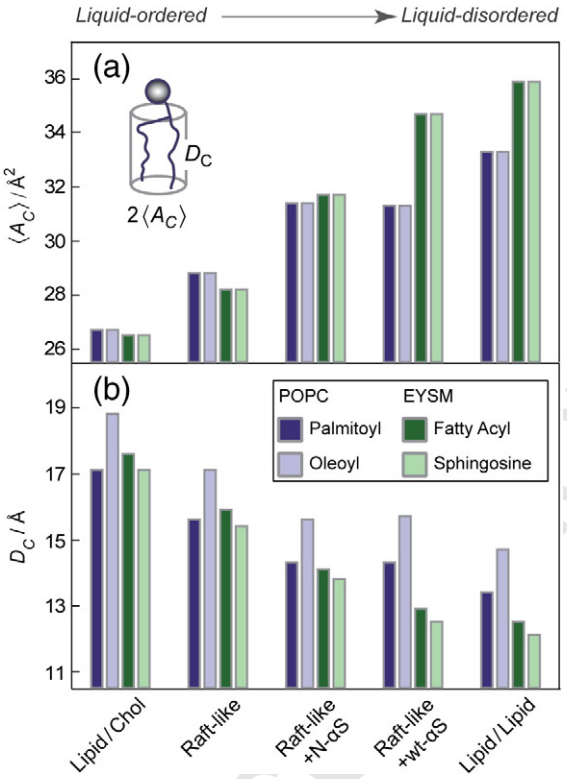

Fig. 8. Mean-torque model yields average cross-sectional areas and hydrocarbon thickness for POPC and EYSM lipids showing αS-induced annealing of raft-like membranes. (a) Average chain cross-sectional area $\langle A_C \rangle$ and (b) volumetric hydrocarbon thickness D_C for indicated mixtures at 48 °C. Both D_C and $\langle A_C \rangle$ are calculated for individual acyl chains, that is, EYSM fatty acyl (*N*-palmitoyl) and sphingosine chains, and POPC palmitoyl and oleoyl chains. Structural parameters for binary POPC/EYSM (1:1), POPC/Chol (1:1), and EYSM/Chol (1:1) membrane support the proposed l_o–l_d structural change of ternary POPC/EYSM/Chol (1:1:1) membranes in the presence of wt-αS and N-αS. Thinning of D_C and an increase of $\langle A_C \rangle$ in the αS-perturbed ternary system characterize the membrane annealing process.

For raft-like membrane phospholipids in the presence of N-αS, the value of D_C for POPC is reduced to 14.3 Å for the palmitoyl chain and 15.7 Å for the monounsaturated oleoyl chain. Hydrocarbon thicknesses of the EYSM fatty acyl and sphingosine chains are 14.1 Å and 13.8 Å, respectively. The corresponding bilayer thickness estimates are found to be D_B = 49.4 Å for POPC and D_B = 42.2 Å for EYSM at 48 °C. An overall reduction of bilayer thickness is accompanied by an increase in cross-sectional area per phospholipid. We find that for POPC, the cross-sectional area per phospholipid is $\langle A \rangle$ = 62.8 Å^2 at 48 °C, which is similar to $\langle A \rangle$ = 63.4 Å^2 in the case of EYSM. These relatively large values indicate that peptide association with the membrane perturbs the stabilizing interactions between lipids, giving rise to thinned bilayers and disordered lipids.

Likewise, the wt-αS protein changes the membrane thickness and cross-sectional area per phospholipid of POPC and EYSM. At 48 °C, the values of D_C for the nonequivalent chains of POPC are 14.3 Å (palmitoyl) and 15.7 Å (oleoyl), whereas values of D_C for EYSM are 12.9 Å and 12.5 Å for the fatty acyl and sphingosine chains. The bilayer thickness D_B =

Please cite this article as: Leftin, A. *et al.*, Solid-State ^{13}C NMR Reveals Annealing of Raft-Like Membranes Containing Cholesterol by the Intrinsically Disordered Protein α-Synuclein, *J. Mol. Biol.* (2013), http://dx.doi.org/10.1016/j.jmb.2013.04.002

ARTICLE IN PRESS

Q2

49.4 Å for POPC is the same as that determined for the N-αS system, while for EYSM, D_B = 39.8 Å, indicating further perturbation. A cross-sectional area of POPC $\langle A \rangle$ = 62.8 Å^2 is found, as in the N-αS system, while the even more pronounced decrease of EYSM bilayer thickness is accompanied by an increase of cross-sectional area to $\langle A \rangle$ = 69.4 Å^2. These results point to an additional interaction of the wt-αS protein with EYSM. This is attributed to differences in the biophysical properties of the glycerolipids and sphingolipids. One difference is the ability of wt-αS to undergo interfacial interactions at sphingosine backbone sites through electrostatics and hydrogen bonding. Such interactions are not available to POPC at the glycerol backbone. Nevertheless, the structural changes observed for both phospholipids show that significant disordering of the bilayers occurs. Large cross-sectional areas per phospholipid and small hydrocarbon thicknesses are found that resemble the binary POPC/EYSM membranes presented in Fig. 8. The mechanism by which disruption of local molecular sites gives rise to these structural rearrangements involves membrane annealing and is discussed below.

Discussion

Annealing of raft-based heterogeneity in lipid membranes by αS

A molecular understanding of Parkinson's disease requires delineation of αS interactions with biomembranes implicated in the processes of neurodegeneration. The protein αS undergoes multiple binding modes, principally initiated at the amphipathic N-terminus,[16,66] with small unilamellar vesicles that are synaptic vesicle models,[16,56,57,66,71–77] as well as large vesicles that mimic the plasma membrane.[73,78] In the physiological system, both of these neuronal membrane targets are highly heterogeneous, which is attributed to differences in membrane composition and phase.[72,79–81] This heterogeneity is especially pronounced for raft-like mixtures where cholesterol interacts differently with POPC and EYSM,[48] resulting in compositionally distinct microdomains, albeit in a similar ordered phase.[43] Lateral compositional heterogeneity gives rise to defects within the membrane that facilitate protein binding, as indicated by a membrane-initiated coil–helix transition of both wt-αS and N-αS.[16,18,19] These defects expose headgroup and backbone sites to solvent and protein.[82] The associated RDCs and S_{CH} order parameter values for headgroup and backbone sites for the POPC/EYSM/Chol (1:1:1) membrane mixture yield striking changes through binding of αS to the bilayer.

The proposed restructuring of the raft-like membrane mixture observed using solid-state ^{13}C NMR is shown schematically in Fig. 1. Here, EYSM and POPC exist in condensed ordered regions in association with cholesterol. In the raft-like membrane mixture, interfacial interactions between lipids and cholesterol prevent lateral diffusion and self-mixing of lipids,[83] leading to a compositionally heterogeneous lateral distribution in so-called domains. Nanometer-scale demixing of locally enriched POPC/Chol and EYSM/Chol ordered complexes, which is unresolved in fluorescence microscopy of this raft-like system,[43] is indicated by different values of the hydrocarbon thickness and average cross-sectional area of the phospholipids. This separation is attributed to local differences in interfacial electrostatics, hydrogen bonding, and differences in hydrophobic volume and length between the membrane components, for example, hydrocarbon mismatch. Interfacial defects between these complexes likely involve mixed POPC/EYSM/Chol regions as indicated in Fig. 1.

Antagonism of αS with cholesterol in raft-like membranes

We propose that αS counters the condensing effect of cholesterol within the raft-like membrane through annealing of the lipid regions. This is a process whereby a material is softened and homogenized through external perturbation, leading to a lower energy state. Disruption of stabilizing lipid packing interactions promotes lateral lipid diffusion[84] and disorders the membrane system. Such a rearrangement is suggested by the increase in average cross-sectional area and reduction of hydrocarbon thickness as the lipid domains are disrupted. Moreover, the chemical shift spectra reveal a homogenization of hydrophobic environment of the membrane. We propose that the annealing likely involves αS–lipid interactions with the negatively charged phosphodiester moiety of the zwitterionic phosphocholine headgroup and partially negative hydrogen-bond acceptor sites of the sphingomyelin backbone. These sites can promote transient association of the protein and peptide with the membrane, leading to the site-specific ^{13}C chemical shift and RDC changes of the headgroup and backbone sites of the phospholipids. Additional interactions with interfacial hydrogen bonding cholesterol sites may play a role in the attraction of αS to the membrane interface, but these effects are not directly observed in our experiments due to the inefficiency of the INEPT magnetization transfer in the DROSS pulse sequence. We have shown previously that amphipathic N-terminal membrane binding initiates a protein conformational change.[16] Our NMR observations also show that while the N-αS peptide inserts to a greater extent into the membrane,

UNCORRECTED PROOF

Please cite this article as: Leftin, A. *et al.*, Solid-State ^{13}C NMR Reveals Annealing of Raft-Like Membranes Containing Cholesterol by the Intrinsically Disordered Protein α-Synuclein, *J. Mol. Biol.* (2013), http://dx.doi.org/10.1016/j.jmb.2013.04.002

ARTICLE IN PRESS

wt-αS causes a more pronounced perturbation of the raft-like membrane environment, due to differences in partition coefficient of the two species related to additional interaction sites on the wt-αS protein. It is possible that deep insertion of peptides or proteins within the hydrocarbon bilayer may cause increases of segmental order and lead to erroneous structural conclusions regarding bilayer integrity. However, in our measurements, we resolve an increase of headgroup and backbone order parameters while hydrocarbon chain order reduces upon peptide and protein interaction. Therefore, further structural analysis using these hydrocarbon chain order parameters is warranted. The mean-torque results provide estimates of the bilayer structural dimensions, thereby identifying a striking shift of coexisting l_o phase regions to a more l_d-like phase in the raft-like membrane. Such effects are not unexpected, since as an amphipathic protein[16,85] αS shares this feature in common with various antimicrobial peptides.[62] These peptides also perturb the membrane interface and induce changes in the hydrophobic membrane center.[86–89] In general, the disruption of stabilizing interfacial interactions and compositional homogenization enables membrane thinning, with a concomitant increase of phospholipid cross-sectional area that can modulate spontaneous membrane curvature.[90–93] While these remodeling properties of the membrane are not specific to αS, it is likely that in the context of synaptic membranes and neurotransmission, such interactions may play a significant role.

The site-specific ^{13}C NMR results show that annealing in raft-like membranes by αS involves interfacial lipid interaction and removes so-called defects. This is consistent with the hypothesis that αS eliminates interfacial fusion sites associated with compositional heterogeneity, thus reducing the probability of fusion events. This function is suggested by our *in vitro* results and is demonstrated in recent *in vivo* studies, where the inhibition of raft-like mitochondrial membrane fusion has been shown in cultured cells and *Caenorhabditis elegans*.[7] Additional biochemical evidence suggesting that αS plays a role in exocytotic membrane fusion comes from the observation of specific association of the C-terminus of αS with a critical subunit of the SNARE fusion complex (synaptobrevin), in conjunction with αS N-terminal membrane interaction.[94] The protein–lipid interaction assists in SNARE complex assembly,[94] thereby facilitating subunit tethering to lipid vesicle membranes. The process is highly dependent on the presence of arachidonic acid,[95] a polyunsaturated fatty acid precursor to many intracellular and extracellular signaling molecules. It is interesting to note that the plasma-membrane-associated SNARE fusion complex requires raft-like membranes enriched in cholesterol and sphingomyelin.[13,15] Localization and function of the protein complex are determined by the balance of liquid-disordered and liquid-ordered phases[96] that in light of our results can be modulated by αS binding.

Conformational plasticity of αS in neural function and dysfunction

Importantly, the conformational plasticity of αS is likely to be critical to its function in membrane lipid fusion and neurodegeneration. Fusion events are highly dynamic, whereby the protein is required to respond rapidly and reversibly to changes in membrane phase,[19] shape,[78] and electrostatic environment.[16] Such interactions have been identified as contributing to the biasing of conformational ensembles of αS. Our results reveal membrane perturbations caused by αS that further emphasize the importance of raft-like, compositionally heterogeneous membranes as an important target for this intrinsically disordered protein.[11] Not only are the structural states of the protein perturbed in this interaction, but the properties of the membrane are also changed. We find that such an interaction occurs with raft-like membrane mixtures through specific association with interfacial lipid sites, which propagates large-scale structural deformation throughout the hydrophobic acyl chain region. These physical changes may modulate fusion, either directly through changes in the membrane strain and lipid distribution[91,97] or indirectly by altering lateral lipid mobility that in turn influences membrane protein localization and organization. In this context, the inherent flexibility of αS interaction with biomembranes can be altered by protein aggregation into toxic oligomeric species, eventually leading to impairment of neuronal signaling. The relation of protein plasticity and biomembrane remodeling is an important aspect that can aid in understanding neurological dysfunction implicated in the etiology of Parkinson's disease. How such membrane-dependent mechanisms are related to the aggregation propensity of αS and neurodegeneration and whether similar mechanisms are operative in other neurodegenerative disorders such as Alzheimer's disease are important topics for future research.

Materials and Methods

Sample preparation

POPC and EYSM [predominant species *N*-(palmitoyl)-sphing-4-enine-1-phosphocholine] were from Avanti Polar Lipids Inc. (Alabaster, AL). Cholesterol was procured from Sigma-Aldrich (St. Louis, MO). Monomeric wt-αS was a gift from Drs. Frits Kamp and Christian Haass, University of Münich, Germany, and the N-αS peptide (1–25) was from Primm Biotech, Inc. (Cambridge, MA). Multilamellar lipid vesicle dispersions were prepared from lyophilized powder hydrated with ^2H_2O at pH ≈ 7 (Cambridge Isotopes,

UNCORRECTED PROOF

Please cite this article as: Leftin, A. *et al.*, Solid-State ^{13}C NMR Reveals Annealing of Raft-Like Membranes Containing Cholesterol by the Intrinsically Disordered Protein α-Synuclein, *J. Mol. Biol.* (2013), http://dx.doi.org/10.1016/j.jmb.2013.04.002

ARTICLE IN PRESS

Q2

Cambridge, MA). Additional buffering was not used, thus avoiding salt-screening effects on the αS–lipid interactions. Peptides and proteins were co-added at a low 1:250 molar ratio of N-terminal equivalents of αS to total lipid, so as to limit protein aggregation and study changes of the lipid membranes caused by the protein in its monomeric state. We have shown previously[16] that binding of the protein and of the N-terminal peptide to small unilamellar vesicles is saturated (99% and 97%, respectively) at a total molar ratio of 167 lipids per protein (peptide). A direct determination of thermodynamic binding constants using multilamellar systems and the 1:250 protein/lipid ratio described in this article was not feasible, but is likely on the order of that observed previously. The multilamellar vesicle dispersion was then subjected to 3–5 freeze–thaw–mixing cycles. Lipid samples were tested for ester hydrolysis before and after the experiments by thin-layer chromatography with $CHCl_3$/MeOH/H_2O (65:30:5), followed by charring with 40% H_2SO_4 in EtOH.

Solid-state NMR spectroscopy

Solid-state MAS NMR experiments were conducted using a narrow bore 11.7-T AVANCE-I spectrometer system (Bruker BioSpin Corporation, Billerica, MA). The SLF experiment DROSS[22] was implemented with the Bruker Topspin software platform. A triple-channel MAS NMR probe (DSI-733; Doty Scientific Inc., Columbia, SC) was used for all experiments. Samples were loaded in 40-μL sealing cells and placed in 4-mm thin-wall zirconium rotors. Radio frequency pulses for ^{1}H and ^{13}C channels were adjusted to exactly the same duration, 3.5 μs for the 90° pulses. Dipolar recoupling at 8 kHz MAS spinning frequency was achieved with a chemical shift offset of ε = 0 and anisotropy scaling of χ_p = 0.393.[22,98] Rotor-synchronized sampling of the indirect dimension (t_1) was implemented using the States method with a total of 64 to 128 points.[22] The sampling of the direct time dimension (t_2) was achieved using 8192 points recorded with an interval of 10 μs under 50-kHz ^{1}H SPINAL-32 decoupling.[99] Recycle times were 3 s, with 500–5000 transients averaged for each t_2 value, giving total experiment times ranging from 0.5 to 5 days. The rotor spin rate was controlled to ±2 Hz using a Doty Scientific Inc. spin-rate controller. Temperatures reported are accurate to ±1 °C. The ^{13}C NMR chemical shifts were referenced to TMS (external).

Fourier transformation of the t_1 and t_2 traces was conducted using the Bruker Topspin software and analyzed using Sparky.[100] A 10-Hz exponential broadening was applied to the t_2 domain data while a 50- to 250-Hz Gaussian apodization was applied in the F_1 frequency domain, following zero-filling to 128 points and Fourier transformation of the t_1 dimension. Chemical shift assignments were based on standard additivity and stereochemistry relations contained in the ChemDraw (PerkinElmer Informatics Inc.) database that assumes isotropic conditions and does not include the possibility of residual anisotropic shifts due to incomplete averaging under MAS. Magnetic dipolar couplings were extracted from the F_1 recoupled lineshapes either by direct inspection of peak-to-peak splittings or by lineshape simulations.[22,25] Fits to ^{13}C SLF-DROSS magnetic dipolar lineshapes were generated for ^{13}C–^{1}H spin systems using Topspin and Matlab (MathWorks, Natick, MA) by assuming an axially symmetric Pake lineshape.[101,102] The ^{1}H offset and chemical shift anisotropy were taken to be zero,[22] as justified by the experimental lineshapes. The extracted RDC values were interpreted as ^{13}C–^{1}H NMR segmental order parameters and were calculated from the relation $S_{CH} = \Delta\nu_D/\chi_D\chi_p = 1/2\langle 3\cos^2\beta - 1\rangle$, where $\Delta\nu_D$ is the measured RDC, $\chi_D = (-\gamma_H\gamma_C\hbar/2\pi)\langle r^{-3}\rangle$ is the magnetic dipolar coupling constant (20,395 Hz) for the ^{13}C–^{1}H bond evaluated at the θ = 90° orientation of the lineshape (Pake powder pattern), and χ_p = 0.393 is the pulse sequence scaling factor.[22] An equilibrium averaged internuclear ^{13}C–^{1}H distance of $\langle r^{-3}\rangle^{-1/3}$ = 1.14 Å corrected for dynamic effects[103] was assumed. The values of the magnetic dipolar couplings were found to be consistent over repeated experiments, with random errors being outside of the three significant figures permitted by the calculation of segmental order parameters.

Phospholipid structure calculations

The volumetric hydrocarbon thickness per acyl chain D_C and average cross-sectional area per phospholipid chain $\langle A_C\rangle$ were evaluated from the segmental order parameters S_{CH} using the mean-torque structural model.[31,104] Specifically, the order parameters for C3 of the palmitoyl and oleoyl chains were used for POPC calculations, and the S9 and C5 methylene S_{CH} values were used for the sphingosine and fatty acyl chains of EYSM (see Supplementary Data). Briefly, the cross-sectional area per acyl chain was calculated as $\langle A_C\rangle = q2V_{CH_2}/D_M$, where q is the area factor,[31] D_M = 2.54 Å is the average inter-methylene distance, and V_{CH_2} is the temperature-dependent methylene volume. The volumetric hydrocarbon thickness per acyl chain was $D_C(T) = V_C(T)/\langle A_C\rangle$, in which $V_C(T)$ is the acyl chain volume at temperature T as obtained from the methylene volume V_{CH_2}, the methyl volume $V_{CH_3}\approx 2V_{CH_2}$, and the methine volume $V_{CH}\approx V_{CH_2}/1.31$.[31] The effective membrane thickness D_B was $D_B = 2D_C^{max} + 2D_H$, where D_C^{max} is the maximum acyl chain length calculated for either of the two chains of the asymmetric phospholipid, and D_H is the contribution of the headgroup plus backbone segments to the thickness. For sphingomyelin, $D_H \approx 7$ Å,[105] and for glycerophospholipids such as POPC, $D_H \approx 9$ Å[106] as determined from small-angle X-ray scattering electron densities.

Acknowledgements

We thank L. Ahlstrom, T. Alam, T. Bartels, T. Molugu, and D. Warschawski for discussions. C. Haass and F. Kamp generously provided wild-type αS. Support of this research from the Arizona Biomedical Research Commission and the U.S. National Institutes of Health is gratefully acknowledged.

Supplementary Data

Supplementary data to this article can be found online at http://dx.doi.org/10.1016/j.jmb.2013.04.002

UNCORRECTED PROOF

ARTICLE IN PRESS

Received 23 December 2012;
Received in revised form 14 March 2013;
Accepted 2 April 2013

Keywords:
magic-angle spinning;
membrane lipid raft;
Parkinson's disease;
residual dipolar coupling;
segmental order parameter

Present address: A. Leftin, Department of Chemical Physics, Weizmann Institute of Science, Rehovot 76100, Israel.

Abbreviations used:
2D, two-dimensional; αS, α-Synuclein; Chol, cholesterol; DROSS, dipolar recoupling on-axis with scaling and shape preservation; MAS, magic-angle spinning; N-αS, N-terminal α-Synuclein (1–25); POPC, 1-palmitoyl-2-oleoyl-*sn*-glycero-3-phosphocholine; RDC, residual dipolar coupling; SLF, separated local-field; wt-αS, wild-type α-Synuclein.

References

1. de Lau, L. M. L. & Breteler, M. M. B. (2006). Epidemiology of Parkinson's disease. *Lancet Neurol.* **5**, 525–535.
2. Dauer, W. & Przedborski, S. (2003). Parkinson's disease: mechanisms and models. *Neuron*, **39**, 889–909.
3. Eliezer, D., Kutluay, E., Bussell, R., Jr & Browne, G. (2001). Conformational properties of alpha-synuclein in its free and lipid-associated states. *J. Mol. Biol.* **307**, 1061–1073.
4. Lotharius, J. & Brundin, P. (2002). Pathogenesis of Parkinson's disease: dopamine, vesicles and α-synuclein. *Nat. Rev. Neurosci.* **3**, 932–942.
5. Cookson, M. R. (2005). The biochemistry of Parkinson's disease. *Annu. Rev. Biochem.* **74**, 29–52.
6. Beyer, K. (2007). Mechanistic aspects of Parkinson's disease: α-synuclein and the biomembrane. *Cell Biochem. Biophys.* **47**, 285–299.
7. Kamp, F., Exner, N., Lutz, A. K., Wedner, N., Hegermann, J., Brunner, B. *et al.* (2010). Inhibition of mitochondrial fusion by α-synuclein is rescued by PINK1, Parkin and DJ-1. *EMBO J.* **29**, 3571–3589.
8. Südhof, T. C. (2004). The synaptic vesicle cycle. *Annu. Rev. Neurosci.* **27**, 509–547.
9. Jensen, P. H., Nielsen, M. S., Jakes, R., Dotti, C. G. & Goedert, M. (1998). Binding of α-synuclein to brain vesicles is abolished by familial Parkinson's disease mutation. *J. Biol. Chem.* **273**, 26292–26294.
10. Kahle, P. J., Neumann, M., Ozmen, L., Müller, V., Jacobsen, H., Schindzielorz, A. *et al.* (2000). Subcellular localization of wild-type and Parkinson's disease-associated mutant a-synuclein in human and transgenic mouse brain. *J. Neurosci.* **20**, 6365–6373.
11. Fortin, D. L., Troyer, M. D., Nakamura, K., Kubo, S., Anthony, M. D. & Edwards, R. H. (2004). Lipid rafts mediate the synaptic localization of α-synuclein. *J. Neurosci.* **24**, 6715–6723.
12. Takamori, S., Holt, M., Stenius, K., Lemke, E. A., Gronbørg, M., Riedel, D. *et al.* (2006). Molecular anatomy of a trafficking organelle. *Cell*, **127**, 831–846.
13. Pfrieger, F. W. (2003). Role of cholesterol in synapse formation and function. *Biochim. Biophys. Acta*, **1610**, 271–280.
14. Edidin, M. (2003). The state of lipid rafts: from model membranes to cells. *Annu. Rev. Biophys. Biomol. Struct.* **32**, 257–283.
15. Rohrbough, J. & Broadie, K. (2005). Lipid regulation of the synaptic vesicle cycle. *Nat. Rev. Neurosci.* **6**, 139–150.
16. Bartels, T., Ahlstrom, L. S., Leftin, A., Kamp, F., Haass, C., Brown, M. F. & Beyer, K. (2010). The N-terminus of the intrinsically disordered protein α-synuclein triggers membrane binding and helix folding. *Biophys. J.* **99**, 2116–2124.
17. Braun, A. R., Sevscik, E., Chin, P., Rhoades, E., Tristram-Nagle, S. & Sachs, J. N. (2012). a-Synuclein induces both positive mean curvature and negative Gaussian curvature in membranes. *J. Am. Chem. Soc.* **134**, 2613–2620.
18. Nuscher, B., Kamp, F., Mehnert, T., Odoy, S., Haass, C., Kahle, P. J. & Beyer, K. (2004). α-Synuclein has a high affinity for packing defects in a bilayer membrane: a thermodynamics study. *J. Biol. Chem.* **279**, 21966–21975.
19. Kamp, F. & Beyer, K. (2006). Binding of α-synuclein affects the lipid packing in bilayers of small vesicles. *J. Biol. Chem.* **281**, 9251–9259.
20. Kamp, F. & Hamilton, J. A. (2006). How fatty acids of different chain length enter and leave cells by free diffusion. *Prostaglandins Leukot. Essent. Fatty Acids*, **75**, 149–159.
21. Leftin, A. (2011). An NMR data base for simulations of membrane dynamics. *Biochim. Biophys. Acta*, **1808**, 818–839.
22. Gross, J. D., Warschawski, D. E. & Griffin, R. G. (1997). Dipolar recoupling in MAS NMR: a probe for segmental order in lipid bilayers. *J. Am. Chem. Soc.* **119**, 796–802.
23. Hong, M., Schmidt-Rohr, K. & Nanz, D. (1995). Study of phospholipid structure by ^{1}H, ^{13}C, and ^{31}P dipolar couplings from two-dimensional NMR. *Biophys. J.* **69**, 1939–1950.
24. Hong, M., Schmidt-Rohr, K. & Pines, A. (1995). NMR measurement of signs and magnitudes of C–H dipolar couplings in lecithin J. *Am. Chem. Soc.* **117**, 3310–3311.
25. Warschawski, D. E. & Deveaux, P. F. (2005). Order parameters of unsaturated phospholipids in membranes and the effect of cholesterol: a ^{1}H–^{13}C solid-state NMR study at natural abundance. *Eur. Biophys. J.* **34**, 987–996.
26. Dvinskikh, S. V., Castro, V. & Sandström, D. (2005). Efficient solid-state NMR methods for measuring heteronuclear dipolar couplings in unoriented lipid membrane systems. *Phys. Chem. Chem. Phys.* **7**, 607–613.
27. Dvinskikh, S. V., Dürr, U. H. N., Yamamoto, K. & Ramamoorthy, A. (2007). High-resolution 2D NMR spectroscopy of bicelles to measure the membrane

UNCORRECTED COPY

Please cite this article as: Leftin, A. *et al.*, Solid-State ^{13}C NMR Reveals Annealing of Raft-Like Membranes Containing Cholesterol by the Intrinsically Disordered Protein α-Synuclein, *J. Mol. Biol.* (2013), http://dx.doi.org/10.1016/j.jmb.2013.04.002

ARTICLE IN PRESS

Q2

interaction of ligands. *J. Am. Chem. Soc.* **129**, 794–802.

28. Smith, P. E. S., Brender, J. R. & Ramamoorthy, A. (2008). Induction of negative curvature as a mechanism of cell toxicity by amyloidogenic peptides: the case of islet amyloid polypeptide. *J. Am. Chem. Soc.* **131**, 4470–4478.
29. Brown, M. F. (1996). Membrane structure and dynamics studied with NMR spectroscopy. In *Biological Membranes. A Molecular Perspective from Computation and Experiment* (Merz, K., Jr & Roux, B., eds), pp. 175–252, Birkhäuser, Basel.
30. Bartels, T., Lankalapalli, R. S., Bittman, R., Beyer, K. & Brown, M. F. (2008). Raftlike mixtures of sphingomyelin and cholesterol investigated by solid-state ^{2}H NMR spectroscopy. *J. Am. Chem. Soc.* **130**, 14521–14532.
31. Petrache, H. I., Dodd, S. W. & Brown, M. F. (2000). Area per lipid and acyl length distributions in fluid phosphatidylcholines determined by ^{2}H NMR spectroscopy. *Biophys. J.* **79**, 3172–3192.
32. Williams, G. D., Beach, J. M., Dodd, S. W. & Brown, M. F. (1985). Dependence of deuterium spin–lattice relaxation rates of multilamellar phospholipid dispersions on orientational order. *J. Am. Chem. Soc.* **107**, 6868–6873.
33. Rajamoorthi, K. & Brown, M. F. (1991). Bilayers of arachidonic acid containing phospholipids studied by ^{2}H and ^{31}P NMR spectroscopy. *Biochemistry*, **30**, 4204–4212.
34. Trouard, T. P., Alam, T. M. & Brown, M. F. (1994). Angular dependence of deuterium spin–lattice relaxation rates of macroscopically oriented dilaurylphosphatidylcholine in the liquid-crystalline state. *J. Chem. Phys.* **101**, 5229–5261.
35. Nevzorov, A. A., Trouard, T. P. & Brown, M. F. (1997). Correlation functions for lipid membrane dynamics obtained from NMR spectroscopy. *Phys. Rev. E*, **55**, 3276–3282.
36. Otten, D., Brown, M. F. & Beyer, K. (2000). Softening of membrane bilayers by detergents elucidated by deuterium NMR spectroscopy. *J. Phys. Chem. B*, **104**, 12119–12129.
37. Rajamoorthi, K., Petrache, H. I., McIntosh, T. J. & Brown, M. F. (2005). Packing and viscoelasticity of polyunsaturated w-3 and w-6 lipid bilayers as seen by H-2 NMR and X-ray diffraction. *J. Am. Chem. Soc.* **127**, 1576–1588.
38. Mallikarjuniah, K. J., Leftin, A., Kinnun, J. J., Justice, M. J., Rogozea, A. L., Petrache, H. I. & Brown, M. F. (2011). Solid-state ^{2}H NMR shows equivalence of hyhydration and osmotic pressures in lipid membrane deformation. *Biophys. J.* **100**, 98–107.
39. Gawrisch, K., Eldho, N. V. & Polozov, I. V. (2002). Novel NMR tools to study structure and dynamics of biomembranes. *Chem. Phys. Lipids*, **116**, 135–151.
40. Steinbauer, B., Mehnert, T. & Beyer, K. (2003). Hydration and lateral organization in phospholipid bilayers containing sphingomyelin: a ^{2}H-NMR study. *Biophys. J.* **85**, 1013–1024.
41. Mehnert, T., Jacob, K., Bittman, R. & Beyer, K. (2006). Structure and lipid interaction of *N*-palmitoylsphingomyelin in bilayer membranes as revealed by ^{2}H-NMR spectroscopy. *Biophys. J.* **90**, 939–946.
42. Bunge, A., Muller, P., Stockl, M., Herrmann, A. & Huster, D. (2008). Characterization of the ternary mixture of sphingomyelin, POPC, and cholesterol: support for an inhomogeneous lipid distribution at high temperatures. *Biophys. J.* **94**, 2680–2690.
43. Zhao, J., Wu, J., Shao, H., Kong, F., Jain, N., Hunt, G. & Feigenson, G. (2007). Phase studies of model biomembranes: macroscopic coexistence of Lα + Lβ with light-induced coexistence of Lα + Lo phases. *Biochim. Biophys. Acta*, **1768**, 2777–2786.
44. Veatch, S. L., Soubias, O., Keller, S. L. & Gawrisch, K. (2007). Critical fluctuations in domian-forming lipid mixtures. *Proc. Natl Acad. Sci. USA*, **104**, 17650–17655.
45. Goñi, F. M., Alonso, A., Bagatolli, L. A., Brown, R. E., Marsh, D., Prieto, M. & Thewalt, J. L. (2008). Phase diagrams of lipid mixtures relevant to the study of membrane rafts. *Biochim. Biophys. Acta*, **1781**, 665–684.
46. Marsh, D. (2009). Cholesterol-induced fluid membrane domains: a compendium of lipid-raft ternary phase diagrams. *Biochim. Biophys. Acta*, **1788**, 2114–2123.
47. Ramstedt, B. & Slotte, J. P. (2006). Sphingolipids and the formation of sterol-enriched ordered membrane domains. *Biochim. Biophys. Acta*, **1758**, 1945–1956.
48. Aittoniemi, J., Niemelä, P. S., Hyvönen, M. T., Karttunen, M. & Vattulainen, I. (2007). Insight into the putative specific interactions between cholesterol, sphingomyelin, and palmitoyl-oleoyl phosphatidylcholine. *Biophys. J.* **92**, 1125–1137.
49. Niemela, P. S., Ollila, S., Hyvonen, M. T., Karttunen, M. & Vattulainen, I. (2007). Assessing the nature of lipid raft membranes. *PLoS Comput. Biol.* **3**, e34.
50. Forbes, J., Husted, C. & Oldfield, E. (1988). High-field, high-resolution proton "magic-angle" sample-spinning nuclear magnetic resonance spectroscopic studies of gel and liquid crystalline lipid bilayers and the effects of cholesterol. *J. Am. Chem. Soc.* **110**, 1059–1065.
51. Husted, C., Montez, B., Le, C., Moscarello, M. A. & Oldfield, E. (1993). Carbon-13 "magic-angle" sample-spinning nuclear magnetic resonance studies of human myelin, and model membrane systems. *Magn. Reson. Med.* **29**, 168–178.
52. Villaláin, J. (1996). Location of cholesterol in model membranes by magic-angle-sample-spinning NMR. *Eur. J. Biochem.* **241**, 586–593.
53. Guo, W., Kurze, V., Huber, T., Afdhal, N. H., Beyer, K. & Hamilton, J. A. (2002). A solid-state NMR study of phospholipid–cholesterol interactions: sphingomyelin–cholesterol binary systems. *Biophys. J.* **83**, 1465–1478.
54. van Duyl, B. Y., Ganchev, D., Chupin, V., de Kruijff, B. & Killian, J. A. (2003). Sphingomyelin is much more effective than saturated phosphatidylcholine in excluding unsaturated phosphatidylcholine from domains formed with cholesterol. *FEBS Lett.* **547**, 101–106.
55. Holland, G. P. & Alam, T. M. (2006). Multi-dimensional ^{1}H–^{13}C HETCOR and FSLG-HETCOR NMR study of sphingomyelin bilayers containing cholesterol in the gel and liquid crystalline states. *J. Magn. Reson.* **181**, 316–326.

UNCORRECTED PROOF

Please cite this article as: Leftin, A. *et al.*, Solid-State ^{13}C NMR Reveals Annealing of Raft-Like Membranes Containing Cholesterol by the Intrinsically Disordered Protein α-Synuclein, *J. Mol. Biol.* (2013), http://dx.doi.org/10.1016/j.jmb.2013.04.002

ARTICLE IN PRESS

56. Bisaglia, M., Tessari, I., Pinato, L., Bellanda, M., Giraudo, S., Fasano, M. *et al.* (2005). A topological model of the interaction between α-synuclein and sodium dodecyl sulfate micelles. *Biochemistry*, **44**, 329–339.
57. Bussell, R., Jr, Ramlall, T. F. & Eliezer, D. (2005). Helix periodicity, topology, and dynamics of membrane-associated α-synuclein. *Protein Sci.* **14**, 862–872.
58. Perlmutter, J. D., Braun, A. R. & Sachs, J. N. (2009). Curvature dynamics of α-synuclein familial Parkinson disease mutants: molecular simulations of the micelle- and bilayer-bound forms. *J. Biol. Chem.* **284**, 7177–7189.
59. Jenco, J. M., Rawlingson, A., Daniels, B. & Morris, A. J. (1998). Regulation of phospholipase D2: selective inhibition of mammalian phospholipase D isoenzymes by a- and b-synucleins. *Biochemistry*, **37**, 4901–4909.
60. Han, H., Weinreb, P. H. & Lansbury, P. T., Jr (1995). The core Alzheimer's peptide NAC forms amyloid fibrils which seed and are seeded by beta-amyloid: is NAC a common trigger or target in neurodegenerative disease? *Chem. Biol.* **2**, 163–169.
61. Comellas, G., Lemkau, L. R., Zhou, D. H., George, J. M. & Reinstra, C. M. (2012). Structural intermediates during a-synuclein fibrillogenesis on phospholipid vesicles. *J. Am. Chem. Soc.* **134**, 5090–5099.
62. Henzler-Wildman, K. A., Martinez, G. V., Brown, M. F. & Ramamoorthy, A. (2003). Perturbation of the hydrophobic core of lipid bilayers by the human antimicrobial peptide LL-37. *Biochemistry*, **43**, 8459–8469.
63. Vogel, A., Katzka, C. P., Waldmann, H., Arnold, K., Brown, M. F. & Huster, D. (2005). Lipid modifications of a Ras peptide exhibit altered packing and mobility versus host membrane as detected by ^{2}H solid-state NMR. *J. Am. Chem. Soc.* **127**, 12263–12272.
64. Vogel, A., Tan, K., Waldmann, H., Feller, S. E., Brown, M. F. & Huster, D. (2007). Flexibility of Ras lipid modifications studied by ^{2}H solid-state NMR and molecular dynamics simulations. *Biophys. J.* **93**, 2697–2712.
65. Madine, J., Hughes, E., Doig, A. J. & Middleton, D. A. (2008). The effects of α-synuclein on phospholipid vesicle integrity: a study using ^{31}P NMR and electron microscopy. *Mol. Membr. Biol.* **25**, 518–527.
66. Bodner, C. R., Dobson, C. M. & Bax, A. (2009). Multiple tight phospholipid-binding modes of α-synuclein revealed by solution NMR spectroscopy. *J. Mol. Biol.* **390**, 775–790.
67. Stottrup, B. L., Stevens, D. S. & Keller, S. L. (2005). Miscibility of ternary mixtures of phospholipids and cholesterol in monolayers, and application to bilayer systems. *Biophys. J.* **88**, 269–276.
68. Panda, A. K., Wojciechowski, P., Nag, K., Possmayer, F. & Petersen, N. O. (2009). Thermodynamic and fluorescence studies on the interaction of cholesterol with palmitoyl-oleoyl phosphatidylcholine and sphingomyelin. *J. Disp. Sci. Technol.* **30**, 1255–1261.
69. Calhoun, W. I. & Shipley, G. G. (1979). Fatty acid composition and thermal behavior of natural sphingomyelins. *Biochim. Biophys. Acta*, **555**, 436–441.
70. McConnell, H. M. & Radhakrishnan, A. (2003). Condensed complexes of cholesterol and phospholipids. *Biochim. Biophys. Acta*, **1610**, 159–173.
71. Narayanan, V. & Scarlata, S. (2001). Membrane binding and self-association of α-synucleins. *Biochemistry*, **40**, 9927–9934.
72. Kubo, S., Nemani, V. M., Chalkley, R. J., Anthony, M. D., Hattori, N., Mizuno, Y. *et al.* (2005). A combinatorial code for the interaction of α-synuclein with membranes. *J. Biol. Chem.* **280**, 31664–31672.
73. Rhoades, E., Ramlall, T. F., Webb, W. W. & Eliezer, D. (2006). Quantification of α-synuclein binding to lipid vesicles using fluorescence correlation spectroscopy. *Biophys. J.* **90**, 4692–4700.
74. Drescher, M., Godschalk, F., Veldhuis, G., van Rooijen, B. D., Subramaniam, V. & Huber, M. (2008). Spin-label EPR on α-synuclein reveals differences in the membrane binding affinity of the two antiparallel helices. *ChemBioChem*, **9**, 2411–2416.
75. Ramakrishnan, M., Jensen, P. H. & Marsh, D. (2003). α-Synuclein association with phosphatidylglycerol probed by lipid spin labels. *Biochemistry*, **42**, 12919–12926.
76. Madine, J., Doig, A. J. & Middleton, D. A. (2006). A study of the regional effects of α-synuclein on the organization and stability of phospholipid bilayers. *Biochemistry*, **45**, 5783–5792.
77. Ulmer, T. S., Bax, A., Cole, N. B. & Nussbaum, R. L. (2005). Structure and dynamics of micelle-bound human α-synuclein. *J. Biol. Chem.* **280**, 9595–9603.
78. Ferreon, A. C., Gambin, Y., Lemke, E. A. & Deniz, A. A. (2009). Interplay of α-synuclein binding and conformational switching probed by single-molecule fluorescence. *Proc. Natl Acad. Sci. USA*, **106**, 5645–5650.
79. Perrin, R. J., Woods, W. S., Clayton, D. F. & George, J. M. (2001). Exposure to long chain polyunsaturated fatty acids triggers rapid multimerization of synucleins. *J. Biol. Chem.* **276**, 41958–41962.
80. Sharon, R., Bar-Joseph, I., Frosch, M. P., Walsh, D. M., Hamilton, J. A. & Selkoe, D. J. (2003). The formation of highly soluble oligomers of α-synuclein is regulated by fatty acids and enhanced in parkinson's disease. *Neuron*, **37**, 583–595.
81. De Franceschi, G., Frare, E., Bubacco, L., Mammi, S., Fontana, A. & de Laureto, P. P. (2009). Molecular insights into the interaction between α-synuclein and docosahexaenoic acid. *J. Mol. Biol.* **394**, 94–107.
82. Cui, H. S., Lyman, E. & Voth, G. A. (2011). Mechanism of membrane curvature sensing by amphipathic helix containing proteins. *Biophys. J.* **100**, 1271–1279.
83. Filippov, A., Oradd, G. & Lindblom, G. (2004). Lipid lateral diffusion in ordered and disordered phases in raft mixtures. *Biophys. J.* **86**, 891–896.
84. Lindblom, G. & Orädd, G. (1994). NMR studies of translational diffusion in lyotropic liquid crystals and lipid membranes. *Prog. Nucl. Magn. Reson. Spectrosc.* **26**, 483–515.
85. Bussell, R., Jr & Eliezer, D. (2003). A structural and functional role for 11-mer repeats in a-synuclein and other exchangeable lipid binding proteins. *J. Mol. Biol.* **329**, 763–778.
86. Epand, R. M., Surewicz, W. K., Hughes, D. W., Mantsch, H., Segrest, J. P., Allen, T. M. & Anantharamaiah, G. M.

UNCORRECTED PROOF

Please cite this article as: Leftin, A. *et al.*, Solid-State ^{13}C NMR Reveals Annealing of Raft-Like Membranes Containing Cholesterol by the Intrinsically Disordered Protein α-Synuclein, *J. Mol. Biol.* (2013), http://dx.doi.org/10.1016/j.jmb.2013.04.002

ARTICLE IN PRESS

Q2

(1989). Properties of lipid complexes with amphipathic helix-forming peptides. *J. Biol. Chem.* **264**, 4628–4635.
87. Epand, R. M., Shai, Y., Segrest, J. P. & Anantharamaiah, G. M. (1995). Mechanisms for the modulation of membrane bilayer properties by amphipathic helical peptides. *Biopolymers*, **37**, 319–338.
88. Epand, R. M. & Vogel, H. J. (1999). Diversity of antimicrobial peptides and their mechanisms of action. *Biochim. Biophys. Acta*, **1462**, 11–28.
89. Epand, R. F., Maoly, W. L., Ramamoorthy, A. & Epand, R. M. (2010). Probing the "charge cluster mechanism" in amphipathic helical cationic antimicrobial peptides. *Biochemistry*, **49**, 4076–4084.
90. Lee, A. G. (1977). Annular events: lipid–protein interactions. *Trends Biochem. Sci.* **2**, 231–233.
91. Brown, M. F. (1994). Modulation of rhodopsin function by properties of the membrane bilayer. *Chem. Phys. Lipids*, **73**, 159–180.
92. Chen, F. Y., Lee, M. T. & Huang, H. W. (2003). Evidence for membrane thinning effect as the mechanism for peptide-induced pore formation. *Biophys. J.* **84**, 3751–3758.
93. Mecke, A., Lee, D. K., Ramamoorthy, A., Orr, B. G. & Holl, M. M. B. (2005). Membrane thinning due to antimicrobial peptide binding: an atomic force microscopy study of MSI-78 in lipid bilayers. *Biophys. J.* **89**, 4043–4050.
94. Burré, J., Sharma, M., Tsetsenis, T., Buchman, V., Etherton, M. R. & Südhof, T. C. (2010). α-Synuclein promotes SNARE-complex assembly in vivo and in vitro. *Science*, **329**, 1663–1667.
95. Darios, F., Ruiperéz, V., López, I., Villanueva, J., Gutierrez, L. M. & Davletov, B. (2010). α-Synuclein sequesters arachidonic acid to modulate SNARE-mediated exocytosis. *EMBO Rep.* **11**, 528–533.
96. Bacia, K., Schuette, C. G., Kahya, N., Jahn, R. & Schwille, P. (2004). SNAREs prefer liquid-disordered over "raft" (liquid-ordered) domains when reconstituted into giant unilamellar vesicles. *J. Biol. Chem.* **279**, 37951–37955.
97. Zimmerberg, J. & Kozlov, M. M. (2006). How proteins produce cellular membrane curvature. *Nat. Rev. Mol. Cell Biol.* **7**, 9–19.
98. Tycko, R., Dabbagh, G. & Mirau, P. A. (1989). Determination of chemical shift anisotropy lineshapes in a two dimensional magic angle spinning NMR experiment. *J. Magn. Reson.* **85**, 265–274.
99. Fung, B. M., Khitrin, A. K. & Ermolaev, K. (2000). An improved broadband decoupling sequence for liquid crystals and solids. *J. Magn. Reson.* **142**, 97–101.
100. Goddard, T. D. & Kneller, D. G. SPARKY 3. University of California, San Francisco.
101. Mehring, M. (1983). *Principles of High Resolution NMR in Solids*, 2nd Edit. Springer-Verlag, Heidelberg.
102. Nevzorov, A. A., Moltke, S., Heyn, M. P. & Brown, M. F. (1999). Solid-state NMR line shapes of uniaxially oriented immobile systems. *J. Am. Chem. Soc.* **121**, 7636–7643.
103. Brown, M. F. (1984). Unified picture for spin–lattice relaxation of lipid bilayers and biomembranes. *J. Chem. Phys.* **80**, 2832–2836.
104. Petrache, H. I., Tu, K. & Nagle, J. F. (1999). Analysis of simulated NMR order parameters for lipid bilayer structure determination. *Biophys. J.* **76**, 2479–2487.
105. Maulik, P. R., Atkinson, D. & Shipley, G. C. (1986). X-ray scattering of vesicles of *N*-acyl sphingomyelins. *Biophys. J.* **50**, 1071–1077.
106. Petrache, H. I., Tristram-Nagle, S. & Nagle, J. F. (1998). Fluid phase structure of EPC and DMPC bilayers. *Chem. Phys. Lipids*, **95**, 83–94.

UNCORRECTED PROOF

Please cite this article as: Leftin, A. *et al.*, Solid-State ^{13}C NMR Reveals Annealing of Raft-Like Membranes Containing Cholesterol by the Intrinsically Disordered Protein α-Synuclein, *J. Mol. Biol.* (2013), http://dx.doi.org/10.1016/j.jmb.2013.04.002